force diagonal matrix element in the case of a certain long-range force which gives more weight to interactions at large rather than small distances. The SC model indicates, however, that in certain classes of two-particle states the sign of the matrix element is determined by the particle coupling and does not depend on details of well shapes.

Use of this approximation procedure substantiated the prediction of the SC model that an *attractive* tensor force would *raise* the energy level of any state in class (3). The ability to make this statement depends on the fact that the Racah coefficients in the general matrix-element formula all have a "stretched" triangular condition for all states of class (3). Such Racah coefficients are always positive.

Examination of the tables of coupling schemes for odd-odd nuclei reveals several interesting points.[1,3] In situations where the strong rule is applicable, we find a total of 52 cases. The strong rule fails in five cases. In two of these five cases we have evidence that the tensor interaction plays a vital role.[2] In the 47 cases where the strong rule holds, the SC model can be applied to 11 cases. In these 11 cases the model indicates that the tensor effect may be repulsive in the ground state. Actually the situation is not clear, for in five of these cases one of the particles is in an S state. In the great majority of situations where the strong rule holds, the ground state is mixed in L-S coupling, and the tensor-force effect is probably to lower the energy of the level.

One can make a more definitive statement in the cases where the weak rule applies. Out of 23 cases where the weak rule is applicable, we find that 20 cases have $j_1=l_1+\frac{1}{2}$, $j_2=l_2+\frac{1}{2}$ *rather* than spin and orbital momentum antiparallel for both particles. In these 20 cases, the weak rule would predict that the ground state should be given by the coupling in Eq. (3). We find that in these cases the weak rule holds nine times and fails eleven times. Our discussion shows that an attractive n-p tensor force will raise such a state [Eq. (3)] in energy and thus bias against it being the ground state.

Calculations with zero-range central forces generally show a competition between $J=j_1+j_2$ and $J=|j_1-j_2|$ for the ground state in a weak-rule situation. A recent study[4] has shown that in such a coupling situation the observed ground state is often $J=|j_1-j_2|$ rather than $J=j_1+j_2$ (see also reference 1). The SC model described here shows that an attractive n-p tensor force would produce level shifts tending to move $J=|j_1-j_2|$ downward in energy with respect to $J=j_1+j_2$.

[3] K. Way, D. N. Kundu, C. L. McGinnis, and R. van Lieshout, *Annual Review of Nuclear Science* (Annual Reviews, Inc., Palo Alto, California, 1956), Vol. 6, p. 129.

[4] M. H. Brennan and A. M. Bernstein, Bull. Am. Phys. Soc. **5**, 20 (1960).

PHYSICAL REVIEW VOLUME 119, NUMBER 2 JULY 15, 1960

Photoproton and Photoneutron Production in Aluminum and Copper*

R. E. CHRIEN† AND A. H. BENADE
Case Institute of Technology, Cleveland, Ohio
(Received March 2, 1960)

The ratio of proton to neutron yields from aluminum and copper irradiated with betatron x rays up to 20.8 Mev in energy has been measured. Simultaneous detection of protons and neutrons is accomplished by placing two samples of the same element in series in the x-ray beam. Direct detection methods are used in each case, a shallow proportional counter for protons and a boron-lined detector for neutrons. A photon difference method has been used to reduce yield data to cross-section form. The proton and neutron yields for aluminum are found to be approximately equal at 20 Mev with cross sections of 19 and 21 millibarns, respectively. At 20.8 Mev a yield ratio of one proton to about 6 neutrons is found for copper, with a peak photoproton cross section of 23 millibarns. The results are compared to a calculation based on the assumption that these reactions proceed through the formation of a compound nucleus.

I. INTRODUCTION

ALTHOUGH an abundant literature relating to the subject of photonuclear reactions has been built up in recent years, the preponderance of the available material is concerned with neutron emission, owing to the difficulties involved in the direct detection of photoprotons.[1]

Further information concerning the characteristics of charged particle reactions would be of use for example in investigating the applicability of the compound nucleus concept to photonuclear reactions. The proton energy spectrum and the size of the photoproton cross section relative to the photoneutron cross section

* This report is based upon a thesis submitted by one of us (R.E.C.) in partial fulfillment of the requirements for the degree of Doctor of Philosophy at Case Institute of Technology. This research has been supported by the U. S. Atomic Energy Commission.

† Now at Brookhaven National Laboratory, Upton, New York.

[1] For a concise summary of earlier work in this field, see G. R. Bishop and R. Wilson, in *Handbuch der Physik*, edited by S. Flügge (Springer-Verlag, Berlin, 1957), Vol. XLII, p. 332.

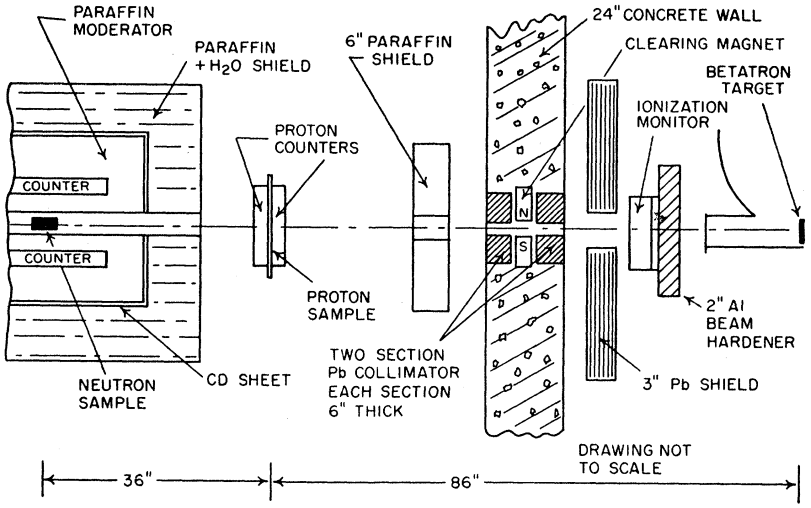

FIG. 1. Experimental arrangement of apparatus. The drawing is not to scale.

can indicate the extent to which the given reaction takes place by way of a compound nucleus. Bishop and Wilson (see reference 1) describe the experimental evidence for the existence of an additional process in which the photon energy is imparted directly to a single nucleon. In high Z elements, the ejection of charged particles by a compound nucleus is inhibited by the large Coulomb barrier, so that in these elements the direct interactions account for most of the observed photoproton yield.

The present investigation seeks to compare the photoproton yield with the photoneutron yield from aluminum and similarly from copper up to about 20 Mev. The experimental results are compared to a calculation of the relative size of these yields under the assumption that the reaction proceeds via the formation of a compound nucleus. The energy dependence of the proton counter efficiency poses several problems in this regard —these will be discussed later on. Photon difference calculations are used to deduce the (γ,n) and (γ,p) cross sections over the same energy interval.

II. DESCRIPTION OF EXPERIMENT

The proton and neutron yields are measured at the same time with detectors arranged in the x-ray beam from the Case betatron as shown in Fig. 1. The proton counter consists of a pair of shallow proportional counters, spaced $\frac{1}{16}$ in apart, between which are inserted sample foils having an area larger than the beam cross section. The counters are equipped with thin Mylar end windows to allow protons to enter the counters from the external sample foil with a small energy loss. The x-ray beam passes through the proton detectors, which are made thin to keep electron production to a minimum. Further details of the proportional counter construction are given in Sec. III.

The proton counting system is followed in the x-ray beam by a neutron detector which consists of a B^{10} lined counter embedded in a paraffin moderator. The paraffin block is surrounded by about 14 inches of paraffin and water shielding to reduce the background from extraneous photoneutrons produced in the betatron vault.

Yield data for neutrons were taken at approximately 0.5-Mev intervals for betatron energies from 20.8 Mev down to neutron threshold. Protons were counted to the lowest energy giving an appreciable counting rate above background. This limiting energy was 8.3 Mev for copper and 11.7 Mev for aluminum. Background runs were cycled with the sample runs at about 15- to 20-minute intervals.

For determining the ratio of proton to neutron yields, no beam monitoring is required since the same beam traverses both detection systems. A copper slug, however, was cycled frequently with the sample in the neutron detection system, and the neutron counting rate from this copper standard was regarded as a monitor of beam intensity. This copper standard was used so that the yield data could be converted to cross-section form. The use of this standard assumes a known x-ray spectrum shape but not an absolute beam intensity. The cross sections for photoproton and photoneutron production in aluminum, and for photoproton production in copper are thus determined relative to an assumed copper photoneutron cross section.

The principal difficulty in an attempt to count photoprotons during the betatron burst is caused by pile-up of electron pulses in the detector. Almost all of these electrons arise in the aluminum or copper sample foils, the contribution from the counter walls and grids being negligible. Electrons which traverse both counters produce substantially identical signals at the two inputs of the preamplifier-subtractor circuit (see Fig. 3). These two signals are subtracted one from the other to give a null output. The main amplifier and scaler system receives only the *difference* in signal between the two counters, so that a proton traversing one or other of the counters gives rise to an output signal whose polarity

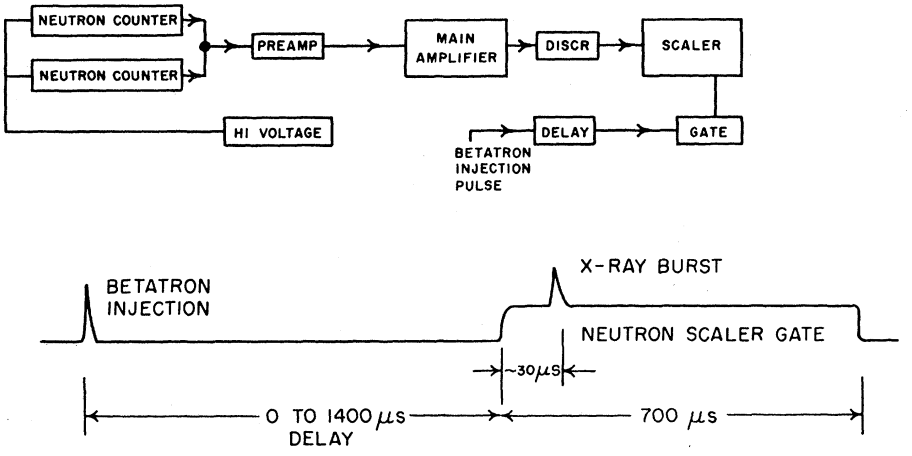

FIG. 2. Block diagram of the electronic apparatus for the neutron channel.

directly implies the proton direction. At the photon energies of interest, electrons are ejected in the forward direction relative to the beam, so that pile-up will chiefly affect the counter furthest from the betatron. Since the photoproton production is expected to be equal in both the forward and backward directions, a consistent inequality in rates from the forward and backward detectors indicates pile-up. Comparison of these two rates can therefore be used as a method of finding the highest beam intensity at which pile-up effects are negligible.

To keep the pile-up within manageable bounds, the betatron burst was lengthened to 15 microseconds by adding a series inductance in the expander circuit, and the proton channel pulse amplifier was set to give a clipping time of 0.2 sec. As a final check, several points on the yield curve were redetermined using a self-expanded betatron burst of about 150-microseconds duration for which pile-up should be vanishingly small. The counting rates were found to agree with the rest of the data, indicating the absence of pile-up effects. With these safeguards it was found possible to expose the samples to a betatron beam having an intensity of about 0.07 r/min.

In order to reduce beam-independent background in both systems, it was found advantageous to gate the neutron and proton channel scalers so that they were on only during an interval around the x-ray bursts. A block diagram of the equipment for the proton and neutron channels and the gating time relationships are shown in Figs. 2 and 3. Calibration procedures for the counters is described below.

III. DESCRIPTION OF DETECTORS

A. Proton Detector

Figure 4 shows a sectional view of one of the two shallow proportional counters used for proton detection in this experiment. The body of the counter is made up of the brass cup "*A*" fastened to the brass plate "*B*"

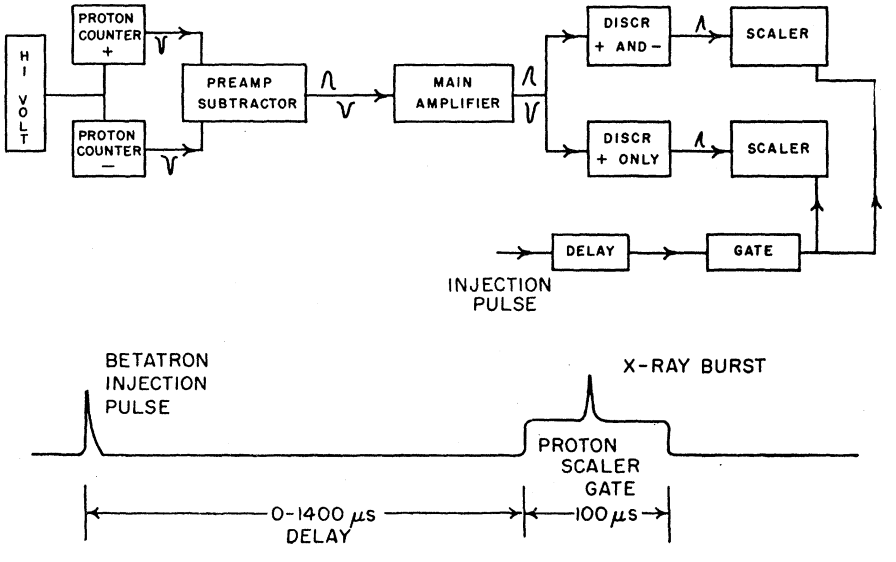

FIG. 3. Block diagram of the electronic apparatus for the proton channel.

by Allen screws. A brass ring centered in the counter supports 8 collector grid wires of 0.001-inch diameter nickel. The grid ring is in turn supported by 3 feed-through terminals which provide the high-voltage connection to the collector. The terminals have guard rings to minimize spurious pulses. Aluminum-coated Mylar foil of 0.00025-inch thickness is used for the counter end windows. A very open grid of 4 wires, held at ground potential, is stretched across the inside of each window to minimize the sensitivity of the internal electric fields to end window movement or "breathing." The axial thickness of the counter, due to gas, windows, and grids, is less than 6 mg/cm^2.

Commercial high purity (99.6%) argon diluted 5% by CO_2 flows continuously through the counters from a pressure regulator followed by a needle valve. The counter could be operated up to 1800 volts, with a gas multiplication up to 200. A solenoid operated arm inserts and removes sample foils from between the counters. Use of the two detectors closely spaced allows the achievement of large geometrical efficiency for counting of protons from the sample foil.

B. Neutron Channel

The neutron detection is accomplished by means of two B^{10} lined proportional counters[2] embedded in a (10×10×18) inch block of paraffin clad with 0.020-inch cadmium. The apparatus has been used and described by Romanowski and Voelker,[3] and has been modified only by the addition of further shielding and a 3 position solenoid-operated target changer.

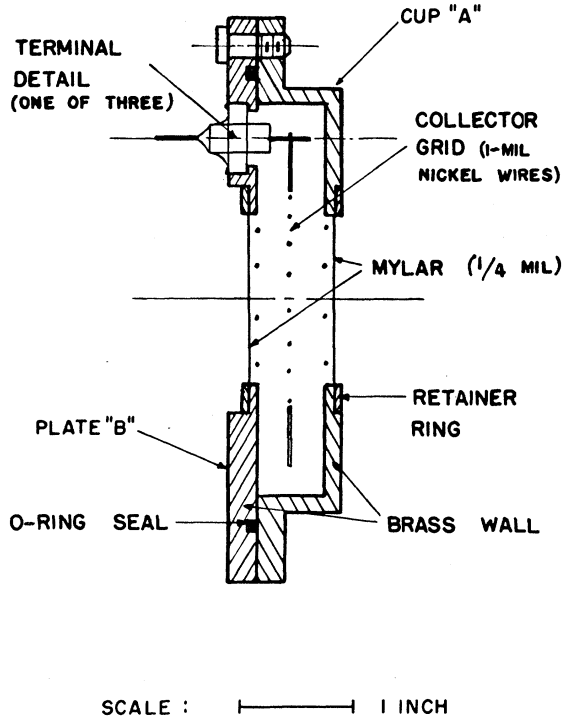

FIG. 4. A cross section view of the proton counter.

[2] AEC BP-7B, General Electric Company.

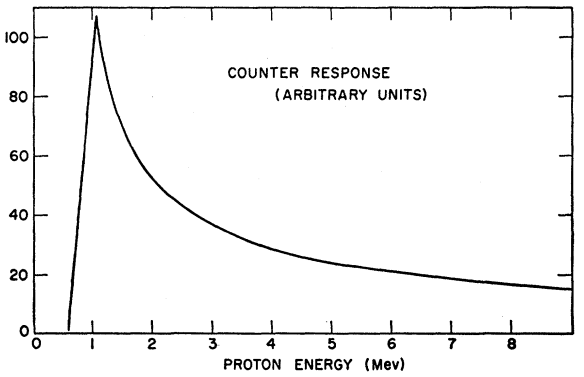

FIG. 5. The pulse-height response of the proton counter to protons of various energies.

IV. CALIBRATIONS

The 5.3-Mev α particle from Po^{210} is used to measure the response of the proportional counter, and for a daily check on its stability. The counter response may be inferred from the observed pulse height produced by α particles with the aid of range-energy relations for protons and for α particles in air, corrected for the stopping power of argon relative to air.[4,5] The relative response of the counter to protons is shown in Fig. 5. This calibration has also been verified with 2.0-Mev protons from the Brookhaven Van de Graaf. The decreasing sensitivity to higher energy is caused by the thinness of the counter.

To determine a discrimination level high enough to bias out electron background, a counting rate curve was obtained with the betatron, using a self-expanded beam at 17.4 Mev on an Al sample foil as shown in Fig. 6. On the basis of this curve the minimum pulse height accepted by the proton channel scaler was set at such a level that protons whose energies lie between 0.7 and 5.0 Mev were detected.

To determine an over-all detection efficiency, the proton energy spectrum must be known at least approximately. Corrections for foil absorption are made by dividing the sample foil into 5 sublayers and computing energy losses for protons originating in the middle of each sublayer, including the angular effect on the path length in the foil. A knowledge of the energy spectrum of protons as they leave the nucleus can be obtained from theory and experiment. Diven and Almy[6] give the following expression for the energy spectrum

[3] T. A. Romanowski and W. H. Voelker, Phys. Rev. **113**, 886 (1959).

[4] *Experimental Nuclear Physics*, edited by E. Segrè (John Wiley & Sons, New York, 1953), Vol. 180.

[5] W. Aron, University of California Radiation Laboratory Report UCRL-121, November, 1948 (unpublished).

[6] B. C. Diven and G. M. Almy, Phys. Rev. **80**, 407 (1950).

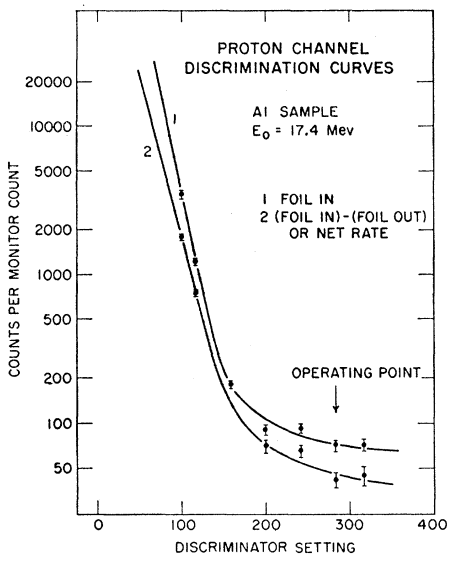

FIG. 6. A bias curve for the proton counter.

of photoprotons emitted from bremsstrahlung-excited nuclei:

$$F(e_p)=e_p\sigma_p\int_{B_p}^{E_0}\sigma_{\gamma n}(E)P(E,E_0)\times\omega_R(E-B_p-e_p)(dE/\Gamma_n), \quad (1)$$

$$\Gamma_n=\int_0^{E_0-B_n}e_n\sigma_n\omega_R(E-B_n-e_n)de_n, \quad (2)$$

where B_p and B_n are the particle binding energies, e_p and e_n the particle energies, σ_n and σ_p the particle capture cross sections, $P(E,E_0)$ the bremsstrahlung spectrum with E_0 the maximum photon energy, and ω_R the level density in the residual nucleus. Furthermore, experimental data for the proton spectra from Cu and Al are available from the work of Diven and Almy on aluminum[6] and from Byerly and Stephens on copper.[7] In the case of copper (1) has been evaluated for $\omega_R=k\exp(aE)^{\frac{1}{2}}$, $a=1.6\ (A-40)^{\frac{1}{2}}$ for 16- and 19-Mev bremsstrahlung, and the resulting over-all proton detection calculated including self-absorption. These efficiencies are found to differ only slightly from that calculated from the experimental distribution of Byerly and Stephens for 24-Mev bremsstrahlung. It is concluded that the over-all detection efficiency for protons from the moderately thick foils used in this experiment is insensitive to the small differences between theoretical and observed spectra, and insensitive to the bremsstrahlung maximum energy within reasonable limits. For the reduction of the present data, the *observed* distributions of Diven and Almy for Al under 20.8-Mev bremmstrahlung and of Byerly and Stephens for Cu under 24-Mev bremsstrahlung are employed. The resulting efficiencies are 0.36 for Al and 0.29 for Cu. The approximate equality of these efficiencies demonstrates the counter insensitivity to photoproton energy distributions under the conditions of this experiment. For the neutron counter a Ra-Be source, standardized against National Bureau of Standards source 38, with a strength of 658±67 neutrons/sec is used for calibration. An efficiency of 0.74% is obtained. Possible differences between the photoneutron and Ra-Be neutron distributions are ignored in view of the energy insensitivity of the Segrè-Wiegand type of neutron detector.

TABLE I. Area densities, atomic numbers, and photon absorption factors for the experimental samples, together with the corresponding particle detection efficiencies.

	Cu (neutrons)	Cu (protons)	Al (neutrons)	Al (protons)
M (mg/cm)	34060	68.12	1290	29.01
A	63.57	63.57	27.0	27.0
ϵ	0.0074	0.287	0.0074	0.360
k	1.667	1.000	1.124	1.000

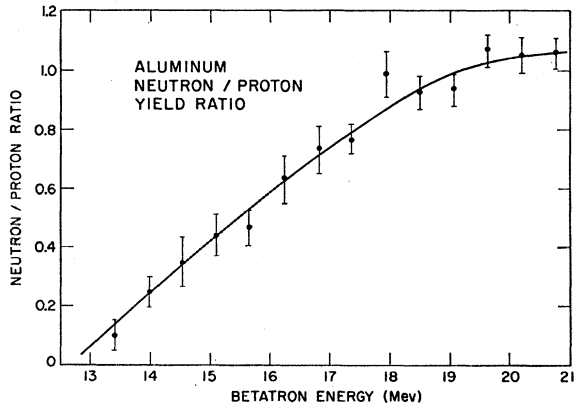

FIG. 7. The photoneutron to photoproton yield ratio for aluminum as a function of betatron energy.

The betatron energy scale was calibrated at three energies, 10.6, 18.73, and 17.0 Mev. The first two points are the photoneutron thresholds for Cu^{63} and C^{12}, calculated from atomic mass data,[8] while the third point was calculated by P. French of this laboratory from data taken with a Compton electron spectrometer.

V. TREATMENT OF DATA

The results of this experiment are in the form of ratios O_x/O_n where O_x represents the sample counting rate (either proton or neutron) and O_n represents the neutron rate from the copper standard. Since all target areas are larger than the x-ray beam area, the following

[7] P. R. Byerly and W. E. Stephens, Phys. Rev. **83**, 54 (1951).
[8] W. H. Sullivan, "Trilinear Chart of the Nuclides," U. S. Atomic Energy Commission, January, 1957 (unpublished).

relation holds,

$$Y_x(E_0)=(O_x/O_n)\left\{N\int_0^{E_0}\sigma_{\mathrm{Cu}}(E)P(E,E_0)dE\right\}$$
$$\times(M_{\mathrm{Cu}}/M_x)(A_x/A_{\mathrm{Cu}})(\epsilon_{\mathrm{Cu}}/\epsilon_x)(k_x/k_{\mathrm{Cu}}), \quad (3)$$

where $Y_x(E_0)$ is the yield in particles/mole/100r, $\{N\int\sigma_{\mathrm{Cu}}PdE\}$ is the assumed Cu neutron yield in neutrons/mole/100r, M the area density in mg/cm^2, A the atomic weight, ϵ the detection efficiency, and k is a correction for photon absorption in the thick neuron samples. For this latter correction the total absorption coefficient for 17.6-Mev photons is used. Table I lists these factors for the samples used in the experiment.

The assumed copper yield is calculated from the cross sections for Cu^{63} and Cu^{65} of Katz and Cameron,[9] and a bremsstrahlung spectrum modified by 2 inches of aluminum beam hardener, as calculated by Rose.[10] The photon difference matrices of Penfold and Leiss, as tabulated by Rose, have been used to transform the

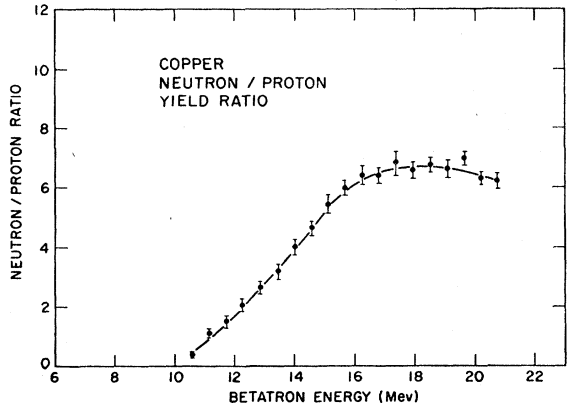

FIG. 8. The photoneutron to photoproton yield ratio for copper as a function of betatron energy.

yield data to cross-section form, after the usual smoothing procedures on the yield curve and its first derivative. These calculations were programmed for, and carried out on the Case IBM 650 computer.

VI. RESULTS AND DISCUSSION

The neutron to proton yield ratios as a function of betatron energy are shown in Figs. 7 and 8 for aluminum and copper, respectively. The principal source of uncertainty in these ratios arises from the calculation of the proton detector efficiency which is influenced by the photoproton energy distribution. However the detection efficiency is not particularly dependent upon the exact shape of the proton energy distribution, as pointed out earlier. This is in part due to the "smearing" effect of the relatively thick samples used in the proportional

[9] L. Katz and A. G. W. Cameron, Can. J. Phys. **29**, 518 (1951).
[10] P. F. Rose, M.S. thesis, Case Institute of Technology, 1956 (unpublished).

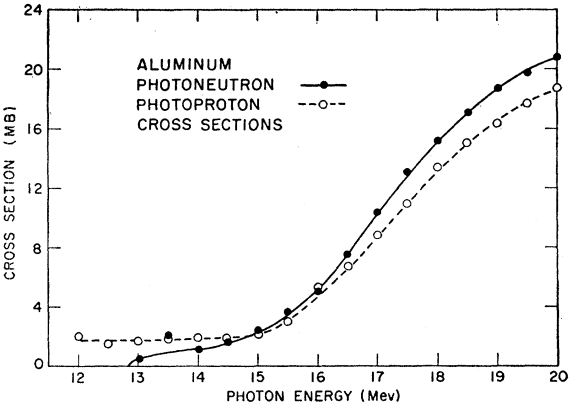

FIG. 9. The photoneutron cross section and the photoproton cross section for aluminum as a function of photon energy.

counter. The insensitivity of our proton detection efficiency to the proton energy spectrum forecloses an effort to measure this spectrum, while at the same time it makes possible a determination of the net yield ratio for comparison with theoretical models.

It should be emphasized that these results are not dependent on beam monitoring since the same beam passes successively through the proton and the neutron samples. The errors shown here are derived from counting statistics only. Figure 9 shows the cross section as a function of photon energy for Al(γ,n) and Al(γ,p), while the Cu(γ,p) cross section appears in Fig. 10. These curves were obtained from the yield data in the manner described in the foregoing section.

The results for Al may be compared to the earlier work of Diven and Almy[6] using an emulsion technique. The present work indicates approximately equal photoneutron and photoproton cross sections at 20 Mev (21 mb for photoneutrons and 19 mb for photoprotons). Diven and Almy used bremsstrahlung of energies 13.9, 17.1, and 20.8 Mev. Using a three-point photon difference method they obtain an average photoproton cross section of 6 mb in the region from 12–20.8 Mev.

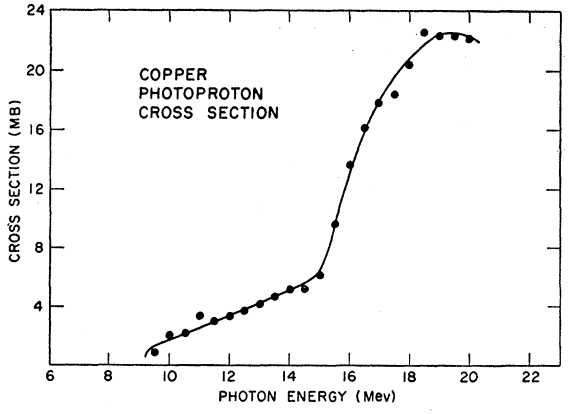

FIG. 10. The photoproton cross section for copper as a function of photon energy.

TABLE II. Calculated ratios of photoproton to photoneutron cross sections.

E_γ (Mev)	Al^{27}	Cu^{63}	Cu^{65}	Cu^{nat}
12	···	0.20	···	0.14
13	···	0.16	0.014	0.11
14	0.83	0.16	0.017	0.11
15	0.54	0.16	0.021	0.12
16	0.44	0.18	0.026	0.13
17	0.39	0.19	0.032	0.14
18	0.35	0.22	0.038	0.17
19	0.32	0.24	0.046	0.18
20	0.30	0.26	0.053	0.20
21	0.28	0.29	0.062	0.22
22	0.27	0.29	0.072	0.23

The present experiment gives 7.6 mb, obtained by averaging the photoproton curve over the same energy region. Montalbetti[11] has measured the aluminum photoneutron cross section by direct detection methods. The present experiment is in substantial agreement with this previously reported value. Halpern and Mann[12] have observed aluminum photoproton yields with a thin zinc sulfide scintillator. Their results are in agreement with the present experiment, although we have obtained the yield curve for photoprotons with considerably better statistical accuracy.

For copper the present experiment indicates a peak cross section for photoproton production of 23 millibarns in the neighborhood of 19 Mev with a yield ratio of about 6 neutrons to one proton at a betatron energy of 20.8 Mev. Copper photoprotons have been observed by Chastel[13] and by Byerly and Stephens[7] with the aid of nuclear emulsions. Chastel employs the lithium 17.6-Mev gamma ray to deduce a photoproton cross section of about 1 mb at that energy, and therefore a photoneutron to photoproton ratio of about 77. Byerly and Stephens report a proton yield of 10^8/mole-100r at 24-Mev betatron energy and a neutron to proton ratio of 4 at that energy. The present experiment is in disagreement with the work of Chastel. Allowing for the difference in betatron energies, the present experimental results seem consistent with those of Byerly and Stephens. The deuteron yield reported by Byerly and Stephens is not expected to be of importance below 20 Mev and has not been taken into account in the present experiment.

The observed ratio of photoproton to photoneutron cross sections may be compared to a calculation of the expected ratio assuming that these photonuclear reactions proceed through the formation of a compound nucleus. Blatt and Weisskopf[14] define a quantity, F_b, which is proportional to the branching ratio for the emission of particle b from the compound nucleus,

$$F_b=(2M_b/\hbar^2)\int_0^{e_m} e\sigma_c(e)\omega_R(e_m-e)de, \qquad (4)$$

where $e_m=E-B_n$, the notation being defined in the discussion following Eq. (1). If the emission is considered to be made up of neutron and proton components only we have:

$$\sigma(\gamma,\mathrm{p})/\sigma(\gamma,n)=F_p/F_n. \qquad (5)$$

The calculation of F involves a knowledge of the neutron and proton cross sections, the respective binding energies and the level densities of the residual nucleus. A level spacing formula due to Newton[15] takes into account the change in effective excitation energy due to pairing effects and also the influence of nuclear shell effects on the level densities. This formula has been used to compute the expected proton to neutron ratios. The capture cross sections are taken from Blatt and Weisskopf, and the binding energies from the nuclear masses quoted by Sullivan,[8] and a recent compilation of Geller, Muirhead, and Halpern.[16] The integral expression is approximated by a finite summation over 0.5-Mev intervals for $Al^{27}(\gamma,n)Al^{26}$, $Al^{27}(\gamma,p)Mg^{26}$, $Cu^{63}(\gamma,n)Cu^{62}$, $Cu^{63}(\gamma,p)Ni^{62}$, $Cu^{65}(\gamma,n)Cu^{64}$, and $Cu^{65}(\gamma,p)Ni^{64}$. The results of this calculation, to 2 significant figures, are given in Table II.

For the case of copper, the agreement between this calculation and our results seems to be quite good, perhaps fortuitously so, considering the approximate nature of the level spacing formula, which has been fitted to nuclides over a wide range of mass numbers. The calculation for aluminum indicates a much lower photoproton to photoneutron ratio than is actually observed. Qualitatively, however, the result does bear out the general expectation that for the lower Z nuclides, with consequently lower Coulomb barriers, the photoproton production is comparable to photoneutron emission.

ACKNOWLEDGMENTS

The authors wish to extend their thanks to Edward Yates for his invaluable assistance in carrying out the experiment, and for the programming of the IBM 650 computer. We are also indebted to A. Hruschka and J. Allen for the mechanical work on the proportional counters.

[11] R. Montalbetti, L. Katz, and J. Goldemberg, Phys. Rev. **91**, 659 (1953).
[12] J. Halpern and A. K. Mann, Phys. Rev. **83**, 370 (1951).
[14] J. Blatt and V. Weisskopf, *Theoretical Nuclear Physics* (John Wiley & Sons, New York, 1952), p. 342.
[15] T. D. Newton, Can. J. Phys. **34**, 804 (1956).
[16] Geller, Muirhead, and Halpern (private communication).